TOWARDS THE CREATION OF SYNTHETIC BRIDGE DIGITAL TWINS WHAT-IF SCENARIOS: STUDY CASE AND CALIBRATION

ALEJANDRO JIMÉNEZ RIOS[1,*], KULTIGIN DEMIRLIOGLU[2], VAGELIS PLEVRIS[3] AND MARIA NOGAL[4]

[1,*] Department of Architecture & Civil Engineering
University of Bath
Bath, BA2 7AY, United Kingdom
e-mail: ajr225@bath.ac.uk, https://orcid.org/0000-0003-4470-255X

[2] Department of Built Environment
Oslo Metropolitan University
NO-0130 Oslo, Norway
e-mail: kultigin@oslomet.no, https://orcid.org/0000-0003-0960-3855

[3] Department of Civil and Environmental Engineering
Qatar University
Doha P.O. Box 2713, Qatar
e-mail: vplevris@qu.edu.qa, https://orcid.org/0000-0002-7377-781X

[4] Department of Materials, Mechanics, Management and Design
Delft University of Technology
2628 CN Delft, The Netherlands
e-mail: m.nogal@tudelft.nl, https://orcid.org/0000-0001-5405-0626

Key words: Finite element method, Calibration, Pre-stressed concrete bridge, Digital twins, FAIR data.

Summary. Digital twins are expected to facilitate the digital transformation of the architecture, construction, engineering, management, operation, and conservation industry. One of their main applications in the field of bridge engineering is the possibility of real-time damage detection. To achieve this, advanced anomaly detection algorithms need to be validated to alert bridge operators on the risks related to the detected anomalies. A synthetic data generation framework has been proposed to generate benchmark databases for testing and validation as a cheaper and faster alternative to the collection of real monitoring data. In this paper we present the S101 Bridge, which has been selected as first case study for the generation of the proposed synthetic database. A finite element model of the bridge was developed and calibrated based on the reported natural frequencies and mode shapes of the actual structure available in the literature. The calibration process is described in detail along with the sensitivity analysis of the considered parameters. The results indicate a strong agreement between the first four natural frequencies and mode shapes of the experimental and numerical bridge model. It is concluded that the calibrated model is suitable for the generation of bride digital twins what-if scenarios, which will be of great significance for both practitioners and the research community.

1 INTRODUCTION

Digital twins (DTs) have been recognized as an enabling technology of the novel Industry 5.0 initiative fostered by the European Union [1]. They represent replicas of physical assets, like bridges, enabling their performance to be supervised and controlled. The creation of a digital twin for a constructed asset allows the different stakeholders of the Architecture, Engineering, Construction, Management, Operation, and Conservation (AECMO&C) industry to track its performance and detect possible damage/decay prior to their escalation into severe problems. This can contribute to enhanced safety and reduced maintenance expenses, particularly in the context of fragile cultural heritage structures, which pose extra challenges due to their unique characteristics and their specific conservation needs [2].

The DT paradigm is nowadays in its early stages of development/adoption within the AECMO&C industry. Nevertheless, and despite all the challenges and constraints that need to be overcome for its full deployment and broad implementation, there appears to be a unified vision and consensus toward the future adoption of DT for bridge design, management, and operation among the scientific community and bridge practitioners [3]. Thus, continued research efforts are essential to establish a well-grounded application framework that can be widely accepted and adopted by the industry. Unfortunately, the collection of experimental and monitoring data is a complex undertaking that requires substantial resources, is susceptible to noise, and may fail to capture representative damage or decay scenarios within the allotted time frame. Other than a few well-known benchmark bridges, i.e., Z24 [4], Dona [5], Vänersborg [6], data are not available for exploitation on open-source databases by researchers working in the field. Furthermore, the data collected through Bridge Health Monitoring (BHM) can be affected by both epistemic and aleatory uncertainties [7] and it is necessary to implement adequate strategies to reduce the estimation error of prediction models using such data [8].

Therefore, the need for a reliable database of benchmark data arises so that new technologies and algorithms can be properly tested and validated within the prototyping stage for bridge DTs. Furthermore, synthetic data used for the creation of "what-if" scenarios for bridge digital twins can provide valuable insights into the bridge's performance under different conditions, allowing AECMO&C professionals to identify potential issues and make informed decisions about maintenance and design challenges. A framework for the creation of a synthetic data generation tool has been proposed [9]. The framework aims at producing high-quality FAIR data that allows novel developed prototypes to be validated and consequently be implemented in further stages of the DT creation for real infrastructure assets. FAIR refers to data that adhere to the principles of findability, accessibility, interoperability, and reusability [10].

Among the features of the synthetic data generation framework are: (i) multi-metric data, namely, vibration, strain, and mixed synthetic data under both undamaged and damaged scenarios, (ii) environmental and operational conditions, (iii) both epistemic and aleatory uncertainties consideration for the adequate generation of real world-like scenarios [11].

In this paper we present the S101 Bridge, which has been selected as first case study for the generation of the proposed synthetic database. A finite element model of the bridge was developed and calibrated based on the reported natural frequencies and mode shapes of the actual structure available in the literature. The calibration process is described in detail along with the sensitivity analysis of the considered parameters. The results indicate a strong agreement between the experimental and numerical bridge calibration results.

2 STUDY CASE DESCRIPTION

The first bridge chosen as a case study for establishing our FAIR database corresponds to the S101 bridge. It represents a typical flyover prestressed concrete bridge, built in the 1960s, in Austria. Due to its poor maintenance condition, insufficient carrying capacity, and incompatible dimensions with modern traffic, the bridge was replaced in the 2000s. However, prior to its demolition, a series of progressive damage tests were conducted on it [12].

More importantly, this bridge is well known among the bridge engineering community and has been used as benchmark by many authors. Moughty and Casas [13] tested on it a vibration based damage detection methodology using the ARMA and Mahalanobis distance algorithms. Limongelli et al. [14] implemented the data-driven Interpolation Method to detect damage in the S101 bridge. On the other hand, Döhler et al. [15] successfully detected the different damages scenarios of the S101 bridge by comparing vibration measurements in a reference state against a damage state through a hypothesis test. More recently, Buckley et al. [16] implemented a supervised machine learning approach and various feature selection method in the S101 bridge study case to identify the minimum set of features capable of providing information to accurately detect damage.

3 GEOMETRY

The dimensions of the different elements were obtained from the case study reported by Wenzel et al. [17]. The resulting geometry is presented in Figure 1, where Figure 1(a) provides a plan view, and Figures 1(b), (c), and (d) depict cross-sections A-A', 1-1', and 2-2', respectively. The bridge deck has a total length of 58 m and a width of 7.2 m. Its main span measures 32 m and every adjacent span measure 12 m (measured from centers of piers and abutments). The bridge was modelled in 3D using the Autodesk AutoCAD 2023 software. The geometry was exported in the IGES format, a format which is compatible with various finite element software packages.

4 NUMERICAL MODELING

To create the numerical model of the S101 bridge first it was needed to import its geometry from the generated IGES file. This was done in the Ansys Workbench software with the use of a Geometry component system. Then, a static structural analysis system was incorporated into the workflow where geometry properties, meshing, boundary conditions, loads, and solver components were defined. Subsequently, a modal analysis system was introduced, inheriting the solution from the static analysis as its setup input.

Figure 2 presents the main components of the developed finite element model. Several concrete materials have been defined using an isotropic elastic constitutive material mode. These materials are assigned to different sections of the bridge deck, each represented by distinct colors in Figure 2. This differentiation allows for tuning their Young's modulus for calibration purposes and simulating diverse damage scenarios. In the model, all four columns are fixed at their bottom, and horizontal displacements are restricted at the bottom faces of the abutments. A vertical spring applied at the lower face of the abutments, considered as one of the inputs parameters for the calibration, completes the set of boundary conditions. Finally, the model is subjected to its own weight (density of 2400 kg/m^3 and standard earth gravity of 9.81 m/s^2) and to a distributed mass per unit area (583 kg/m^2) applied on the side surfaces of the

deck to simulate the weight of the sidewalk and metallic rail of the bridge.
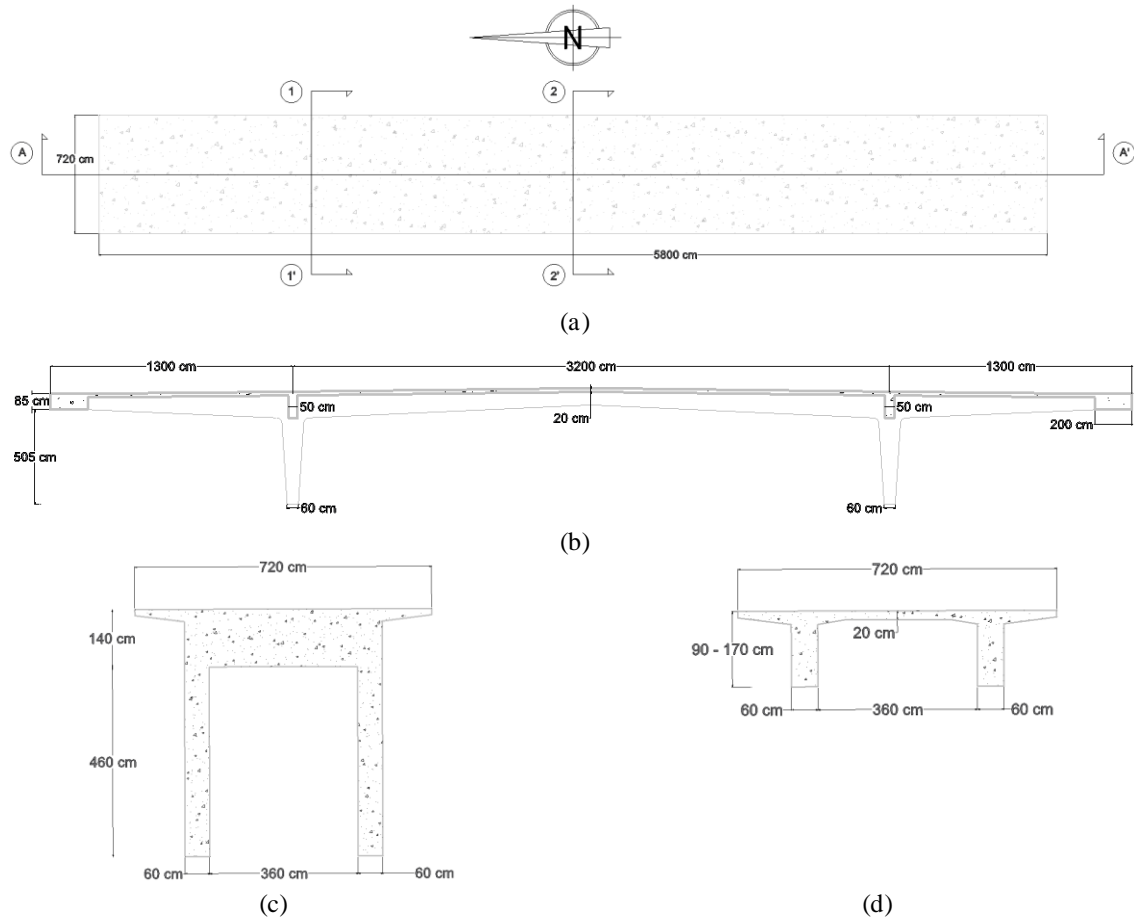

(a)

(b)

(c)   (d)

Figure 1. Bridge geometry: (a) Plan view, (b) Section A-A', (c) Section 1-1', (d) Section 2-2'.
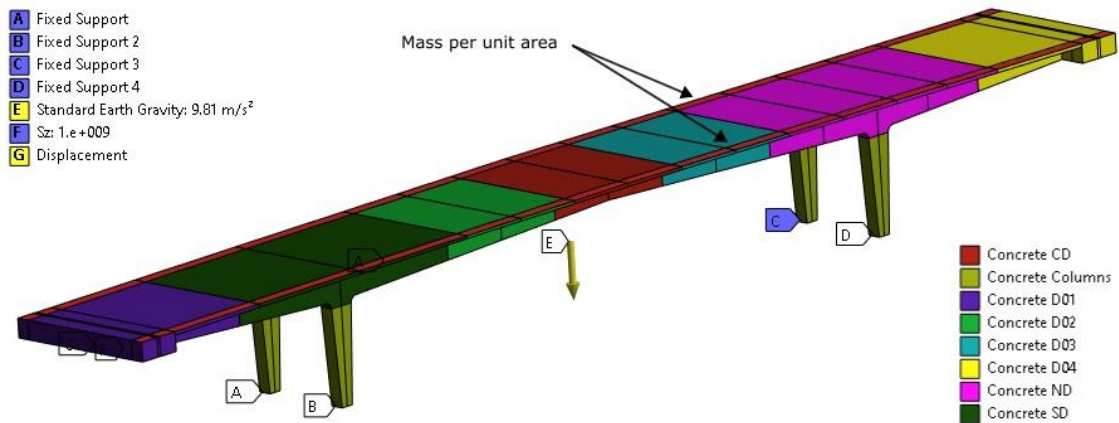

Figure 2. Finite element model set-up supports, loads and material assignments.

The contacts between the different parts of the model were automatically detected by the software and modeled as bonded contacts. A patch conforming algorithm was selected to

4

generate only tetrahedrons for the meshing of the model (SOLID187). This higher order finite element has ten nodes and three degrees of freedom per node (translation in x, y, and z axis).

The modal analysis results (i.e., mode shapes and corresponding frequencies) obtained with the initial finite element model are presented in Figure 3. Figure 3 (a) and (b) present the first and second modes computed with the numerical model, corresponding to the first bending and first torsion modes, respectively. Similarly, Figure 3 (c) and (d) illustrate the fourth and fifth modes, corresponding to the second bending and torsion modes. The third mode of the numerical model has been omitted since it corresponds to a lateral mode shape not captured during the bridge monitoring and subsequent operation modal analysis.
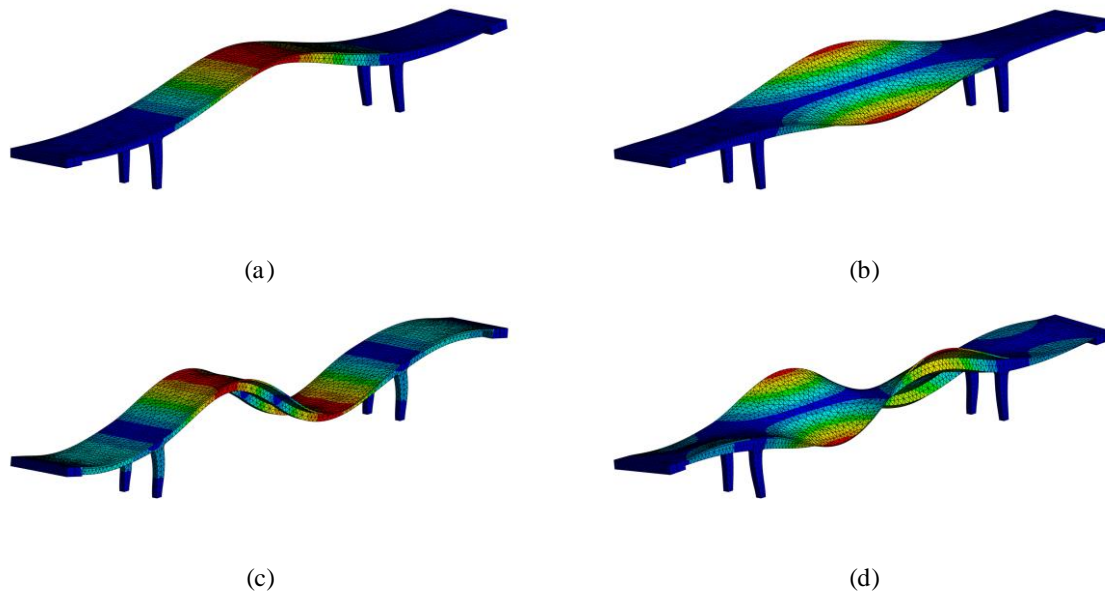

| (a) | (b) |
| (c) | (d) |

Figure 3. Initial numerical modeling results from the modal analysis: (a) First mode shape, F1=3.84 Hz, (b) Second mode shape, F2=5.56 Hz, (c) Fourth mode shape, F4=9.84 Hz, and (d) Fifth mode shape, F5=11.8 Hz.

5 MESH SENSITIVITY ANALYSIS

A mesh sensitivity analysis was performed to make sure that the results would not be significantly affected by the choice of mesh element size. Five different mesh element sizes were analyzed, and the results are presented in Figure 4. These results were obtained using an Ansys Mechanical Enterprise Academic Research solver in a computer with a Windows 10 operating system and with a 12th Gen Intel® Core (TM) i9-12900H processor.

Figure 4 (a) shows the frequency values of the first five modes, derived from numerical models established with various mesh element sizes as indicated in the legend. Notably, the curves exhibit significant overlap, which indicates a low sensitivity in the computed frequency values with respect to the mesh element size. Figure 4 (b) shows both the time to solve (on the left vertical axis) and the average element quality (on the right vertical axis) as a function of the different mesh element size analyzed. Element quality is based on the ratio of the square root of the cube to the sum of the square of the edge lengths for 3D elements. It ranges between 0 and 1, where a value of 1 indicates a perfect cube or square while a value of 0 indicates that the element has a zero or negative volume.
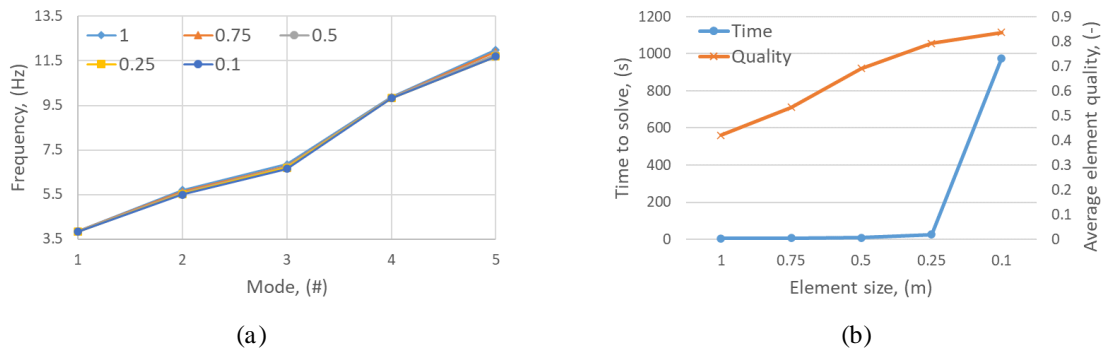
Figure 4. Mesh sensitivity analysis results: (a) Frequency values of the first five modes, (b) Time to solve and average element quality versus mesh element size.

As can be seen, a linear improvement trend in average element quality becomes apparent with a reduction in the element size. However, a notable exponential increase in the time to solve is observed, particularly when the element size is decreased from 0.25 m to 0.1 m. On the other hand, utilizing a 0.25 m element size results in approximately 20% more time required to complete the modal analysis compared to the time obtained with the 0.5 m element size, offering only negligible improvement in average element quality. Consequently, it has been determined that the optimum quality-cost relationship is achieved with a mesh element size of 0.5 m. This size has been consistently used throughout the remainder of this work.

6 MODEL CALIBRATION

6.1 Parameters correlation

First, a correlation analysis of parameters was conducted to identify the model input parameters, which include support stiffnesses and material Young's Modulus, influencing the output parameters, the first five natural frequencies and their corresponding mode shapes considered in this study. This analysis aimed to reduce the computational effort required for the construction of response surfaces and optimization problem. The correlation analysis generated 500 samples by randomly assigning values to the input parameters within specified ranges. Then, the model was solved for every sample and to obtain the corresponding output parameters values. To assess the degree of association between two variables, a Spearman's correlation analysis was performed [18]. Essentially, a high Spearman's correlation implies that observations have a similar or identical rank (correlation of 1) between the two variables, while a low Spearman's correlation suggests that the ranks are dissimilar or entirely opposite (correlation of -1). The results of the Spearman's correlation are graphically presented in Figure 5. It can be seen that CD, ND, and SD are the parameters that better correlate with F1, while ND and SD correlate with F2, and D03-D04 with F4-F5. Sz has a moderate correlation with F4 and F5, whereas "Columns" has a low to moderate correlation with all output parameters. Moreover, from this figure it can be observed that the influence of parameters D01 and D04 is practically negligeable. Therefore, neither D01 nor D04 were considered for the calibration.
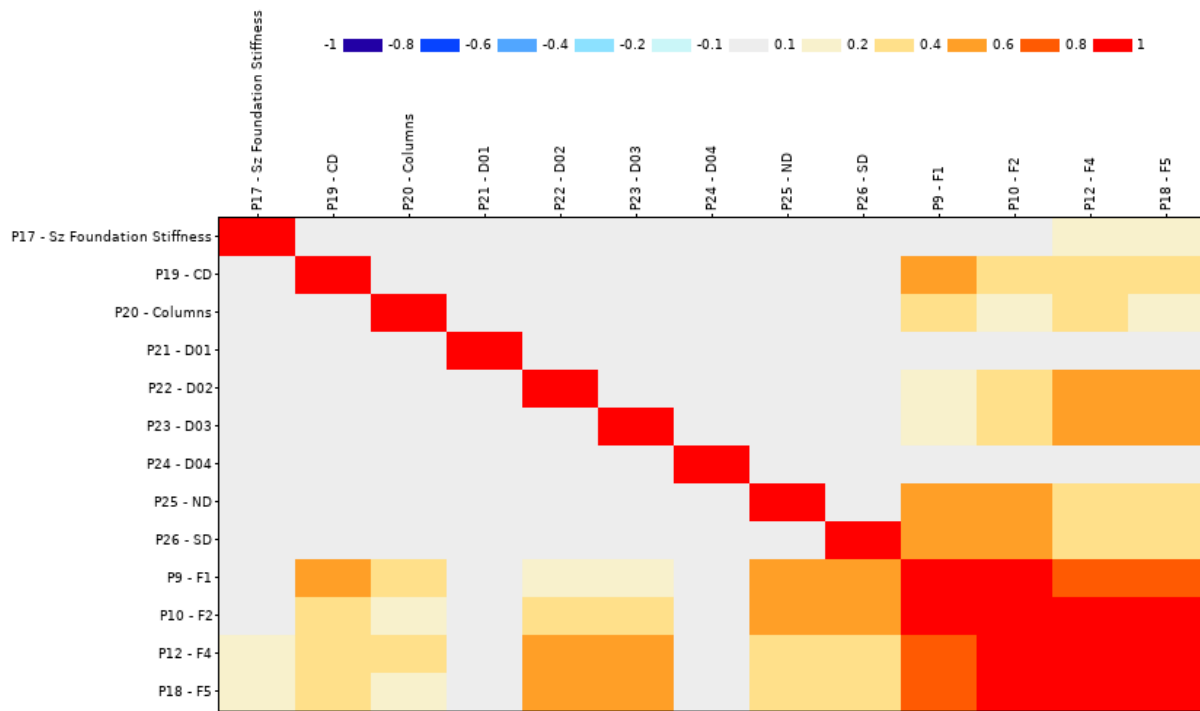
Figure 5. Correlation matrix of Spearman coefficients.

6.2 Response surface optimization

The calibration was conducted through a response surface optimization method. A design of experiments was developed using a Latin Hypercube Sampling Design technique. The samples were created through a Central Composite Design (CCD). This resulted in 79 data points. The information gathered from those analyses was used to create response surfaces following three different approaches, namely, (i) full second order polynomials, (ii) genetic aggregation, and (iii) neural networks. The full second order polynomials method is a well-known statistical methodology used in regression problems. It contains linear, quadratic, and interaction terms and it is relatively simple to understand and interpret. The neural network response surface is a more complex model which consists of interconnected layers of nodes, each performing a simple computation. However, being a black-box model, it can be difficult to understand and interpret in comparison to polynomial models, and it requires larger amounts of data and computational resources for its training. The neural network response surface in this work was built using a simple 7-10-4 architecture (i.e., with 10 nodes in the single hidden layer), due to the inherent lack of model tunning features in the software. Finally, the genetic aggregation technique automatically identifies the most suitable approach to fit each output parameter and build the corresponding response surface. Like neural networks, this method is computationally intensive and may be more difficult to interpret than simpler models.

The value of the spring support was allowed to vary within the range of 1.00E+07 to 1.00E+10 (N/m^3), while the Young's modulus of the different concrete types was within the range from 2.70E+10 to 4.40E+10 (Pa). The second order polynomial optimization was done through manual screening, whereas the ones of the neural network and genetic aggregation optimization were done through a Multi-Objective Genetic Algorithm (MOGA). The values of

the model parameters, established after calibration are presented in Table 1.

Table 1. Values of input parameters after calibration for each response surface optimization methodology.

Parameter	2nd Order Polynomials	Genetic aggregation	Neural Network
Sz (N/m^3)	2.08E+09	7.03E+09	7.39E+09
CD (Pa)	4.31E+10	4.07E+10	4.05E+10
Columns (Pa)	2.86E+10	2.76E+10	3.02E+10
D02 (Pa)	3.49E+10	3.06E+10	2.89E+10
D03 (Pa)	3.73E+10	2.84E+10	2.89E+10
ND (Pa)	4.19E+10	4.33E+10	4.32E+10
SD (Pa)	4.29E+10	4.26E+10	4.32E+10

The frequencies results and their comparison against target values reported from the progressive damage monitoring test of the bridge are presented in Table 2. The best calibration results were provided by the 2nd Order Polynomials response surface approach. All frequency values fell within ± 7% with respect to the target values, and this difference can be considered as the epistemic uncertainty within the foreseen synthetic data generation. The higher Young's modulus value assigned to the ND and SD elements can be explained by the higher stiffness in the nodes where deck and piers connect, as typically observed in this type of bridge typology [19]. The relatively low Young's modulus obtained for the columns could be related to the advanced level of decay detected in the bridge piers during the visual inspection campaign [20]. Furthermore, the first two bending and torsion modes reported from the monitoring tests were well captured with the calibrated numerical model. It is worth noting though, that the third mode of the numerical model corresponded to a lateral bending mode, not captured with the monitoring test. Thus, the third and fourth monitoring modes are compared against the fourth and fifth numerical modes.

7   CONCLUSIONS AND FURTHER WORK

In this paper we presented the S101 Bridge, selected as the first case study for the generation of the proposed synthetic database. A finite element model of the bridge was developed and calibrated based on the reported natural frequencies and mode shapes from a series of monitoring tests. A sensitivity analysis of the model parameters was conducted, and results were used to simplify the subsequent calibration task. The calibration process was conducted following three different response surface optimization approaches. The best calibration was provided by the 2nd Order Polynomials method. The results indicate a strong agreement between the first four natural frequencies and mode shapes of the experimental and numerical bridge model. Furthermore, the values adopted after calibration were briefly described and adequately justified based on a coherent physical interpretation.

The calibrated model will be used to create a FAIR [10] synthetic benchmark database to be used in the development of bridge DT. In addition to the epistemic uncertainty discussed in the calibrated model, the generated data will also encompass aleatory uncertainties and account for

various environmental and operational conditions. Moreover, future work will address and present two additional tasks: self-validation of the generated synthetic data and its ongoing maintenance/support.

Table 2. Frequency values and comparison against target values from the monitoring test in the bridge.

#		1	2	3	4	5
Target	F (Hz)	4.05	6.30	9.69	13.29	15.93
	Type	Bending	Torsion	Bending	Torsion	Bending
2nd Order Polynomials	F (Hz)	4.070	5.890	10.200	12.500	15.400
	Type	Bending	Torsion	Bending (4)*	Torsion (5)*	Bending (6)*
	Difference (%)	0.49	-6.96	5.00	-6.32	-3.44
Genetic Aggregation	F (Hz)	4.01	5.72	9.67	12.00	15.40
	Type	Bending	Torsion	Bending (4)*	Torsion (5)*	Bending (6)*
	Difference (%)	-1.00	-10.14	-0.21	-10.75	-3.44
Neural Networks	F (Hz)	4.04	5.72	9.70	12.00	15.50
	Type	Bending	Torsion	Bending (4)*	Torsion (5)*	Bending (6)*
	Difference (%)	-0.25	-10.14	0.10	-10.75	-2.77

* The number within parenthesis indicates the mode shape number.

REFERENCES

1. European Commission. *Enabling Technologies for Industry 5.0 : results of a workshop with Europe's technology leaders*. 2020 URL: https://data.europa.eu/doi/10.2777/082634.
2. Jiménez Rios, A. and D. O'Dwyer, *External Post-tensioning System for the Strengthening of Historical Stone Masonry Bridges*, in *RILEM Bookseries*. 2019, Springer Netherlands. p. 1566-1574. https://doi.org/10.1007/978-3-319-99441-3_168.
3. Jiménez Rios, A., V. Plevris, and M. Nogal, *Bridge Management through Digital Twin-based Anomaly Detection Systems: A Systematic Review*. Frontiers in Built Environment, 2023 https://doi.org/10.3389/fbuil.2023.1176621.
4. Maeck, J. and G. De Roeck, *Description of Z24 Benchmark*. Mechanical Systems and Signal Processing, 2003. **17**(1): p. 127-131 https://doi.org/10.1006/mssp.2002.1548.
5. Dilena, M. and A. Morassi, *Dynamic testing of a damaged bridge*. Mechanical Systems and Signal Processing, 2011. **25**(5): p. 1485-1507 https://doi.org/10.1016/j.ymssp.2010.12.017.
6. Leander, J., et al., *Dataset for damage detection retrieved from a monitored bridge pre and post verified damage*. Data in Brief, 2023. **51**: p. 109729 https://doi.org/10.1016/j.dib.2023.109729.
7. Peng, T., et al., *Role of Sensors in Error Propagation with the Dynamic Constrained Observability Method*. Sensors, 2021. **21**(9) https://doi.org/10.3390/s21092918.
8. Peng, T., et al., *Planning low-error SHM strategy by constrained observability method*. Automation in Construction, 2021. **127** https://doi.org/10.1016/j.autcon.2021.103707.
9. Jiménez Rios, A., V. Plevris, and M. Nogal, *Synthetic data generation for the creation of bridge digital twins what-if scenarios*, in *9th International Conference on Computational Methods in Structural Dynamics and Earthquake Engineering (COMPDYN)*. 2023: Athens, Greece. https://doi.org/10.7712/120123.10760.21262.
10. Wilkinson, M.D., et al., *The FAIR Guiding Principles for scientific data management and stewardship*. Scientific Data, 2016. **3**(1): p. 160018 https://doi.org/10.1038/sdata.2016.18.

11. Jiménez Rios, A., V. Plevris, and M. Nogal, *Uncertainties in the synthetic data generation for the creation of bridge digital twins*, in *5th International Conference on Uncertainty Quantification in Computational Science and Engineering (UNCECOMP)*. 2023: Athens, Greece. https://doi.org/10.7712/120223.10323.20020.

12. Döhler, M., et al., *Structural health monitoring with statistical methods during progressive damage test of S101 Bridge.* Engineering Structures, 2014. **69**: p. 183-193 https://doi.org/10.1016/j.engstruct.2014.03.010.

13. Moughty, J.J. and J.R. Casas, *Vibration based damage detection techniques for small to medium span bridges: A review and case study*, in *8th European Workshop on Structural Health Monitoring, EWSHM 2016*. 2016. p. 2524-2533. https://www.ndt.net/events/EWSHM2016/app/content/Paper/36_Moughty.pdf.

14. Limongelli, M.P., M. Tirone, and C. Surace, *Non-destructive monitoring of a prestressed bridge with a data-driven method*, in *Health Monitoring of Structural and Biological Systems 2017*, T. Kundu, Editor. 2017, SPIE. https://doi.org/10.1117/12.2258381.

15. Döhler, M., F. Hille, and L. Mevel, *Vibration-Based Monitoring of Civil Structures with Subspace-Based Damage Detection*, in *Mechatronics for Cultural Heritage and Civil Engineering*, E. Ottaviano, A. Pelliccio, and V. Gattulli, Editors. 2018, Springer International Publishing: Cham. p. 307-326. https://doi.org/10.1007/978-3-319-68646-2_14.

16. Buckley, T., B. Ghosh, and V. Pakrashi, *A Feature Extraction & Selection Benchmark for Structural Health Monitoring.* Structural Health Monitoring, 2023 https://doi.org/10.1177/14759217221111141.

17. Wenzel, H., R. Veit-Egerer, and M. Widmann, *Case Study: S101*, in *Industrial Safety and Life Cycle Engineering*. 2013. p. 423-442. https://www.researchgate.net/publication/258925781_Case_Study_S101.

18. Spearman, C., *The Proof and Measurement of Association between Two Things.* The American Journal of Psychology, 1904. **15**(1): p. 72-101 https://doi.org/10.2307/1412159.

19. Gonen, S., K. Demirlioglu, and E. Erduran, *Optimal sensor placement for structural parameter identification of bridges with modeling uncertainties.* Engineering Structures, 2023. **292**: p. 116561 https://doi.org/10.1016/j.engstruct.2023.116561.

20. Wenzel, H., et al. *Integrated European Industrial Risk Reduction System WP3 Demonstration Report*. 2012 URL: https://www.vce.at/iris/pdf/deliverables/D11-1_S101REIT_08-2308_scientific%20modif_extensive_report.pdf.